HHS Public Access

Author manuscript

Reproduction. Author manuscript; available in PMC 2024 August 01.

Published in final edited form as:

Reproduction. 2023 August 01; 166(2): 125–134. doi:10.1530/REP-22-0482.

Peptidylarginine Deiminase 2 Regulates Expression of DGCR8 Affecting miRNA Biogenesis in Gonadotrope Cells

Brett A. Ralston[1,*], **Lamia Khan**[2,*], **Stanley B. DeVore**[3], **Trent A. Bronnenberg**[1], **Joseph W. Flock**[1], **Ari O. Sequoia**[1], **Paul R. Thompson**[4], **Amy M. Navratil**[1], **Brian D. Cherrington**[1]

[1] University of Wyoming, Department of Zoology and Physiology, Laramie, WY 82071, USA

[2] Department of Medicine, Faculty of Medicine and Dentistry, University of Alberta, Edmonton, AB T6G 2R3, Canada

[3] University of Cincinnati College of Medicine, Department of Pediatrics, Cincinnati, OH 45267, USA

[4] University of Massachusetts Medical School, Program in Chemical Biology, Worcester, MA 01605, USA

Abstract

Canonical miRNA biogenesis requires DGCR8 microprocessor complex subunit, which helps cleave pri-miRNAs into pre-miRNAs. Previous studies found that inhibiting peptidylarginine deiminase (PAD) enzyme activity results in increased DGCR8 expression. PADs are expressed in mouse gonadotrope cells, which play a central role in reproduction by synthesizing and secreting the luteinizing and follicle stimulating hormones. Given this, we tested whether inhibiting PADs alters expression of DGCR8, DROSHA, and DICER in the gonadotrope derived LβT2 cell line. To test this, LβT2 cells were treated with vehicle or 1 μM pan-PAD inhibitor for 12 hours. Our results show that PAD inhibition leads to an increase in DGCR8 mRNA and protein. To corroborate our results, dispersed mouse pituitaries were also treated with 1 μM pan-PAD inhibitor for 12 hours which increases DGCR8 expression in gonadotropes. Since PADs epigenetically regulate gene expression, we hypothesized that histone citrullination alters *Dgcr8* expression thereby affecting miRNA biogenesis. LβT2 samples were subjected to ChIP using an antibody to citrullinated histone H3, which shows that citrullinated histones are directly associated with *Dgcr8*. Next, we found that when DGCR8 expression is elevated in LβT2 cells, pri-miR-132 and 212 are reduced while mature miR-132 and 212 are increased suggesting heightened miRNA biogenesis. In mouse gonadotropes, DGCR8 expression is higher in diestrus as compared to estrus, which is the inverse of PAD2 expression. Supporting this idea, treatment of ovariectomized mice with 17β-estradiol results in an increase in PAD2 expression in gonadotropes with a corresponding

Corresponding Author: Brian D. Cherrington, Ph.D., Department of Zoology and Physiology, University of Wyoming, 1000 E. University Ave. #3166, Laramie, WY, 82071, Phone: (307) 206-4845, bcherrin@uwyo.edu.

*Equal contributing first authors

Author Contribution Statement

This manuscript was written by BAR, LK, and BDC while AMN helped with editing and revisions. BAR, LK, SBD, JWF, AOS, and TAB conducted the experiments. PRT contributed reagents and financial support for the project was to BDC.

Declaration of interest

The authors have nothing to declare.

decrease in DGCR8. Collectively, our work suggests that PADs regulate DGCR8 expression leading to changes in miRNA biogenesis in gonadotropes.

In brief:

DGCR8 microprocessor complex, which is important for miRNA biogenesis, is regulated by peptidylarginine deiminase 2 and expression fluctuates in gonadotrope cells across the mouse estrous cycle.

Keywords

peptidylarginine deiminase; citrullination; gonadotrope; DGCR8; miRNA

Introduction

Peptidylarginine deiminases (PADIs or PADs) are a family of enzymes that post-translationally modify arginine converting them to neutrally charged citrulline residues in target proteins (Mohanan et al. 2012). Citrullination alters charge and directly affects the structure and function of proteins important for cell physiology including cytoskeletal architecture, chromatin remodeling, and enzymatic pathways (Gyorgy et al. 2006, Vossenaar et al. 2003). PADs and citrullinated proteins are of growing interest because of their functions in autoimmune diseases like rheumatoid arthritis and lupus, as well as, neurodegenerative disorders (Bicker and Thompson). Equally important, PADs are robustly expressed in female reproductive tissues including the uterus, anterior pituitary, and mammary glands suggesting that this enzyme family is physiologically important for female reproductive health and fertility (Cherrington et al. 2012, Christensen et al. 2022, Horibata et al. 2012, Khan et al. 2016). Despite this, the detailed function of PADs and citrullinated proteins in female reproduction is unclear.

The anterior pituitary gonadotrope cell is a central component of the hypothalamic-pituitary-gonadal axis that underlies all mammalian reproduction. In response to hormonal inputs, gonadotropes synthesizes and secrete the gonadotropins luteinizing hormone (LH) and follicle stimulating hormone (FSH). Our previous work discovered that PAD2 is expressed in the gonadotrope derived LβT2 cell line and in mouse anterior pituitary gonadotrope cells (Khan et al. 2016). PAD2 expression is highest in gonadotropes during the estrus stage of the mouse estrous cycle following the increase in serum E2 and the LH surge, which initiates ovulation. In LβT2 cells, PADs citrullinate arginine residue 2, 8, and 17 on histone H3 tails to epigenetically regulate gene expression (Khan et al. 2016).

MicroRNAs are critical for pituitary development, gonadotropin hormone production, ovulation, and female fertility (Ahmed et al. 2017, Hasuwa et al. 2013). To process miRNAs, cells must express the enzymes necessary for miRNA biogenesis. In gonadotropes, cell-specific deletion of DICER suppresses gonadotropins resulting in fertility defects (Wang et al. 2015). Despite this, not all of the enzymes involved in miRNA biogenesis have been characterized in gonadotrope cells. To help to address this gap in knowledge, we focused on DGCR8, which is required for canonical miRNA biogenesis (Gregory

et al. 2004, Wang et al. 2007), but has not been examined in gonadotrope cells. To form the microprocessor complex, DGCR8 binds with DROSHA, a ribonuclease enzyme. This binding is important for stabilizing DROSHA's RNAse III domain around primary microRNA (pri-miR) transcripts. The microprocessor complex extracts the pre-miRNAs from the pri-miRNAs by performing a double stranded cleavage, removing the stem loop. Following export of the pre-miRNA from the nucleus, DICER creates a single stranded mature miRNA that is loaded into the RNA induced silencing complex (RISC) (Beezhold et al. 2010, Ha and Kim 2014). While this mechanism is important for regulating the stability and translation of multiple mRNAs, the importance of DGCR8 to this process in gonadotropes has not been described.

Changes in the levels of DGCR8 likely effects the biogenesis of all miRNAs, but studies presented here have focused on miR-132 and 212 since they have previously been described in gonadotrope cells. Work by Godoy et al. first showed that LβT2 cells express miRNAs 132 and 212 (miR-132 and 212) (Godoy et al. 2011). Following biogenesis, miR-132 and 212 target the 3' untranslated region (UTR) of Rho GTPase Activating Protein 32 (ARHGAP32) to decrease its expression, which alters LβT2 cell morphology and migration (Godoy et al. 2011). MiR-132 and 212 also regulate expression of the FSHβ subunit by targeting the mRNA of the histone deacetylase sirtuin 1 (SIRT1) (Lannes et al. 2015). Thus, miR-132 and 212 are important for gonadotropin production in LβT2 cells and, potentially, for primary gonadotrope cell function. Given this, it is important to increase our understanding of miRNA biogenesis in gonadotropes.

Materials and Methods

Cell Culture and PAD Inhibitor Treatments

LßT2 cells, a generous gift from Dr. Pamela Mellon (University of California, San Diego), were maintained in DMEM containing 100 U penicillin/ml, 100 µg streptomycin/ml and 10% fetal bovine serum (FBS) (HyClone, Logan, UT, USA). All cells were grown in 5% CO_2 at 37 °C in a humidified environment. The anti-LHβ antibody was obtained from the A.F. Parlow National Hormone and Peptide Program (Cat# AFP344191, RRID:AB_2784507). The PAD inhibitor, biphenyl-benzimidazole-Cl-amidine (BB-ClA) was synthesized as previously described (Knight et al. 2015).

qPCR

LßT2 cells were treated with vehicle (DMSO) or 1 µM BB-ClA or transfected for 48 hours with 25 nM of SMARTpool siRNAs targeting DGCR8 (M-051365–00-0020, Dharmacon, Lafeyette, CO). A custom PAD2 siRNA was purchased from Dharmacon: Sense 5'-CCCGUUCUUUGGCCAGCGCdTdT-3; antisense 5'GCGCUGGCCAAAGAACGGGdTdT-3', along with an ON-TARGET plus non-targeting siRNA #1 control (D-001810–01-05) (DeVore et al. 2018, Khan et al. 2016). Total LβT2 RNA was purified according to the Omega Bio-Tek Total RNA Kit protocol (Omega Bio-Tek, Inc., Norcross, GA). 1 µg of resulting RNA was reverse transcribed using iScript Reverse Transcription Supermix for RT-qPCR (Bio-Rad, Hercules, CA). Complementary DNA was subject to real time qPCR analysis with SYBR Green (Bio-Rad) using

intron-spanning primers: DGCR8 forward 5'-GCCTAAAGACAGTGAAGAACTGG-3', reverse 5'-CATGGATCTGATATGGAGAC-3'; DROSHA forward 5'-GGGACGAAACCGAGCTCTG -3', reverse 5'-GCATAACTCAACTGTGCGGG -3'; DICER forward 5'- CCTCGTCAACTCTGCAAACC-3', reverse 5'- AGTCATAATGAGAACCTGGTGCT-3'; PAD2 forward 5'-TTCCTCACGGCCATTGAGAT-3', reverse 5'-TCGGTCACAATTCACCAGCA-3'; Primary-miRNA-132 forward 5'-CGTCAGCCTGCAAGCCC -3', reverse 5'-AGTAACAATCAAAGCCACGG -3'; Primary-miRNA-212 forward 5'-TCAACTGCGGGCGACGG -3', reverse 5'-CAGTAAGCAGTCTAGAGCCAAGGT -3'. Primers were designed using NCBI Primer BLAST and evaluated by melt curve analysis and generation of a standard curve.

For mature miRNA analysis, cells were treated as described above but miRNAs were purified per the Omega Bio-Tek E.Z.N.A. miRNA kit (Omega Bio-Tek, Inc.) protocol. MiRNAs were reverse transcribed using the TaqMan microRNA reverse transcription kit (Thermo Scientific) and small-RNA-specific stem-loop primers that were pooled according to Applied Biosystem's user bulletin PN 4465407 primer pool protocol. TaqMan probes for mmu-miR-132 (assay identifier 461735_mat, catalog number 4427975) and mmu-miR-212–5p (assay identifier 461768_mat, catalog number 4427975) with U6 (4427975) serving as the reference control were purchased from Thermo Scientific. Data was analyzed using the ΔΔCt method where Ct values of targets were adjusted to corresponding Ct values of a reference gene (GAPDH or U6). Experiments were repeated at least 3 independent times and values are expressed as the mean ± SEM. Statistically significant means were identified using Student's t-test and * indicates significantly different means (* $p<0.05$ and ** $p<0.01$).

Western Blotting

LßT2 cells were treated with vehicle or 1μM BB-ClA for 12 hours. Protein lysate concentration was measured by Pierce 660 nm protein assay (Thermo Fisher Scientific Inc., Waltham, MA, USA) prior to gel loading to ensure equal protein loading. Sample buffer consisting of 0.5 M Tris-HCl (pH 6.8), 60% glycerol, 30 mM DTT, 6% SDS was added to samples to yield a final concentration of 1X and then boiled at 95 °C for 5 minutes. The samples were subjected to SDS-PAGE using 12% gels (acrylamide:bis-acrylamide ratio of 29:1) and subsequently transferred to Immobilon PVDF membranes (MiliporeSigma Burlington, MA, USA). Membranes were blocked in 1X casein (Vector Labs, Burlingame, CA, USA) diluted in Tris buffered saline (TBS) containing 0.1% Tween-20 (TBS-T) overnight at 4 °C. An anti-DGCR8 antibody (ab191875, Abcam, Cambridge, MA, USA) or an anti-β-tubulin antibody (T8328, MiliporeSigma), were incubated 1:1000 overnight at 4 °C. The following morning, membranes were washed in TBS-T, followed by a 2 hour incubation at room temperature with 1:10,000 goat anti-rabbit HRP (Jackson ImmunoResearch Labs, West Grove, PA, USA) secondary antibody. All blots were washed for 50 min (5×10 min) with TBS-T after secondary antibody incubation and then visualized using SuperSignal West Pico and Femto chemiluminescence substrate (Thermo Fisher Scientific Inc.). Quantitative densitometry analysis was conducted with Bio-Rad Image Lab software. The experiments were repeated at least three independent times and values are

expressed as the mean ± SEM. Means were separated using Student's t-test and * indicates significantly different means (* $p<0.05$).

Immunocytochemistry (ICC) and immunofluorescent imaging

LβT2 cells were plated in MatTek Life Sciences 35 mm glass-bottom dishes (Ashland, MA, USA). After being fixed in 4% paraformaldehyde and permeabilized, cells were incubated with the same DGCR8 antibody listed above diluted 1:250 overnight at 4 °C, and duplicate dishes were incubated with an equal mass of non-specific rabbit IgG as a negative control. The following morning dishes were washed 3X in PBS before incubation with a fluorophore conjugated secondary antibody, then stained with DAPI. Cells were imaged using a Zeiss 710 or 980 LSM confocal microscope under a 63X objective. Primary pituitary cells from female mice between 8 and 16 weeks of age were collected and dispersed as previously described (DeVore et al. 2018, Navratil et al. 2007). Cells were plated in MatTek Life Sciences 35 mm glass-bottom dishes overnight then treated with vehicle or BB-ClA as described above. Whole mouse pituitaries were collected during the estrus and diestrus stages of the cycle based on vaginal cytology, fixed in 4% paraformaldehyde, placed in 20% sucrose, and frozen at −80 °C. The pituitaries were then sliced on a cryostat into 10 μm sections and placed on charged slides. Dispersed cells and pituitary sections were incubated with an anti-DGCR8 antibody and an anti-LHβ antibody overnight at 4 °C. Controls were incubated with an equal mass of non-specific rabbit IgG as a negative background control. The samples were washed before incubation with a fluorophore conjugated secondary antibody, then stained with DAPI. Intensities of PAD2 in whole cells and DGCR8 in only the nuclei of gonadotropes was quantified using ImageJ by calculating the corrected total cell fluorescence (CTCF) (Schneider et al. 2012). Dispersed cells and pituitary sections were imaged on a Zeiss 710 or 980 LSM confocal microscope. Values are expressed as the mean ± SEM, and means were separated using Student's t-test (* $p<0.05$).

Chromatin Immunoprecipitation (ChIP)

LβT2 cells were treated with either vehicle or 1 μM BB-ClA for 12 hours then cross-linked at room temperature (RT) in 1% formaldehyde for 10 minutes. ChIP was performed with a SimpleChip® Plus Enzymatic Chromatin IP Kit following the manufacturer's protocol (Cell Signaling Technologies, Danvers, MA, USA) and optimized for LβT2 cells. The chromatin was immunoprecipitated using an anti-Histone H3Cit 2,8,17 antibody (ab5103, Abcam) while non-specific rabbit IgG from the kit was used as a control as previously described (DeVore et al. 2018). Enriched DNA was then subjected to qPCR using DGCR8 ChIP primers; forward 5'-CGCCACAGGTAGGTGC-3', reverse 5'-ACGTCCGTGATGCCTGG-3'. Enrichment of citrullinated histones associated with the mouse *Dgcr8* gene was calculated using the percent input method and is shown as vehicle compared to BB-ClA treated cells. The ChIP experiments were performed 3 independent times and was analyzed using Student's t-test (* $p<0.05$)

Mouse Pituitary Tissue

FVB mice were maintained on a 12 h light/dark cycle with *ad libitum* access to food and water. Estrous cycle staging was assessed by vaginal cytology as previously described (Khan et al. 2016). Whole pituitaries from female mice during estrus and diestrus were frozen for

imaging or dispersed as previously described (DeVore et al. 2018, Khan et al. 2016, Navratil et al. 2007). Female mice were ovariectomized and allowed to recover from surgery for one week. Mice received a single intraperitoneal injection with vehicle (vegetable oil) or 20 μg of 17β-estradiol for 12 hours. Following treatment, pituitaries were examined for PAD2 and DGCR8 mRNA and protein expression as described above. Euthanasia was performed by CO_2 asphyxiation and tissue harvested in accordance with the guidelines outlined in the Report of the AVMA on Euthanasia. All work in this study was approved by the University of Wyoming Institutional Animal Care and Use Committee (protocol #20190301BC00345–03, approval April 28, 2021).

Statistical Analysis

All experiments were repeated independently at least three times and resulting values are expressed as the mean ± SEM. Statistical analysis was determined using Excel 2016 (Microsoft, Redmond, WA) or GraphPad Prism 6.0 (GraphPad Software, San Diego, CA). Means were separated using Student's t-test and * indicates significantly different means (* $p<0.05$ and ** $p< 0.01$).

Results

PAD Inhibition or siRNA Mediated Knockdown Alters DGCR8 mRNA and Protein Expression in LβT2 cells

We first tested if PAD inhibition regulates expression of DGCR8, DROSHA, and DICER, the major components of canonical miRNA biogenesis. LβT2 cells were treated with vehicle (DMSO) or 1 μM of the pan-PAD inhibitor, biphenyl-benzimidazole-Cl-amidine (BB-ClA) for 12 hours. Results show that there is an increase in DGCR8 expression following PAD inhibition as compared to vehicle treated cells, but not similar increases in DROSHA or DICER (Figure 1A). We next confirmed that DGCR8 protein levels are elevated following PAD inhibition. Equal amounts of lysates were examined by western blot using an anti-DGCR8 antibody with anti-ß-tubulin as the loading control. A representative western blot and quantification of multiple blots demonstrate that DGCR8 protein expression is increased by approximately 2-fold in BB-ClA treated cells compared to controls (Figure 1B). This observation was further corroborated by confocal microscopy imaging studies, which show an increase in DGCR8 in the nuclei of cells treated with BB-ClA as compared to controls (Figure 1C).

To verify the PAD inhibitor studies by another means, endogenous PAD2 expression in LβT2s was depleted using siRNAs. LβT2 cells were transfected for 48 hours with 25 nM non-targeting control or PAD2 siRNAs and then PAD2 and DGCR8 mRNA was quantified. Compared to cells transfected with non-targeting controls, there is a 40% knockdown of endogenous PAD2 in LβT2 cells with a concurrent small increase in DGCR8 mRNA (Figure 1D). These results demonstrate that in LβT2 cells, knockdown of PAD2 increases DGCR8 expression suggesting that PAD2 catalyzed citrullination regulates its expression.

Citrullinated Histones are Directly Associated with the *Dgcr8* Gene Promoter

We next examined if citrullinated histones are directly associated with the mouse *Dgcr8* gene. Following vehicle or inhibitor treatment, LβT2 cells were lysed and chromatin was immunoprecipitated using an anti-histone H3Cit 2,8,17 antibody or non-specific IgG as previously described (DeVore et al. 2018). The primers target the region +58 to +281 relative to the transcriptional start site of the main *Dgcr8* transcript as annotated by NCBI and was chosen based on the presence of activating histone H3K27 acetylation in the region. PAD inhibition results in a decrease in enrichment of citrullinated histones on *Dgcr8* as compared to vehicle treated controls (Figure 2).

PAD Inhibition and DGCR8 Knockdown Alter miRNA 132 and 212 Biogenesis

Since inhibiting PAD activity or knocking down PAD2 increases DGCR8 expression, we next hypothesized that this would increase miRNA biogenesis resulting in decreased pri-miRNAs as they are converted to pre- and mature miRNAs. MiRs-132 and 212 were examined as proxies for DGCR8 activity in miRNA biogenesis since they have documented expression and function in LβT2 cells and rodent gonadotropes (Godoy et al. 2011, Lannes et al. 2016, Lannes et al. 2015). LβT2 cells were treated with vehicle or 1 μM BB-ClA and then pri-miR-132 and 212 were examined by qPCR (Godoy et al. 2011). PAD inhibition leads to a decrease in pri-miR-132 and 212 transcripts and corresponding increase in mature isoforms suggesting that changes in DGCR8 affect miRNA biogenesis (Figure 3A). As a control, we also examined whether changes in pri-miR-132 and 212 occur when DGCR8 is knocked down in LβT2 cells. LβT2 cells were transfected with 25 nM DGCR8 siRNA or a non-targeting siRNA control for 48 hours, which results in a 40% decrease in endogenous DGCR8 mRNA (Figure 3B). When DGCR8 is knocked down, there is an increase in pri-miR-132 and 212 and lower mature isoforms as compared to the non-targeting controls (Figure 3B). Collectively, these data suggest that modulating DGCR8 expression alters the conversion of pri-miRNAs to mature miRNAs in LβT2 cells.

PAD Inhibition Increases DGCR8 Expression in Dispersed Mouse Gonadotropes

To validate our findings, we quantified DGCR8 expression in mouse pituitary cells following PAD inhibition. Pituitary cells were dispersed, plated, and then treated following the same paradigm used with LßT2 cells. Supporting our LβT2 results, BB-ClA treatment of mouse pituitary cells results in an increase in DGCR8 mRNA (Figure 4A). To determine if the increase in DGCR8 occurs in gonadotropes specifically, dispersed pituitaries cells were treated as described above and then probed with anti-DGCR8 and anti-LHβ antibodies, which specifically labels gonadotrope cells, or an equal concentration of non-specific IgG. DGCR8 expression was quantified in gonadotrope nuclei by normalizing treatments to a non-specific IgG control using ImageJ to generate the corrected total cell fluorescence (CTFC). Representative images and quantification demonstrate that DGCR8 increases in primary gonadotrope nuclei following BB-ClA treatment as compared to controls supporting that PADs regulate expression of DGCR8 (Figure 4B).

DGCR8 Expression in Mouse Gonadotropes is Highest during Diestrus

Previous studies by Qiao *et al.* found that DGCR8 mRNA in mouse gonadotropes is highest in diestrus correlating with the estrous cycle stage in which PAD2 expression is lowest (Khan et al. 2016, Qiao et al. 2016). To investigate this interesting observation, female mouse pituitaries were collected during estrus and diestrus and then PAD2 and DGCR8 mRNA was quantified. In pituitaries collected in estrus, PAD2 expression is elevated while DGCR8 is reduced compared to pituitaries from diestrus (Figure 5A). We next examined DGCR8 protein expression in mouse gonadotropes during estrus and diestrus. Gonadotropes were identified in pituitary sections by staining with an anti-LHβ antibody. Quantification of DGCR8 in the nuclei of LHβ positive gonadotropes shows that expression is higher in diestrus as compared to the estrus pituitary samples (Figure 5B). Thus, not only does inhibiting PADs increase DGCR8 in dispersed pituitary cells, but expression in female mouse gonadotropes is the inverse of PAD2 (Khan et al. 2016). Lastly, it is important to point out that DGCR8 appears to be expressed in almost all dispersed pituitary cells and cells in pituitary sections, which supports a role for this riboprotein in canonical miRNA biogenesis and cellular function.

17β-estradiol Treatment of Ovariectomized Mice Increases PAD2 Expression in Gonadotropes with a Concurrent Decrease in DGCR8

Our previous work shows that PAD2 expression in mouse uteri is stimulated by 17β-estradiol (E2) treatment (Horibata et al. 2012). Thus, we next examined whether vehicle or E2 treatment of ovariectomized mice increases PAD2 expression with a corresponding decrease in DGCR8 in gonadotrope cells. One week post-surgery, mice were inject with vehicle or 20 μg of E2. After 12 hours, pituitaries were collected and examined for PAD2 or DGCR8 mRNA and protein expression. E2 treatment results in an increase in PAD2 expression with a concurrent decrease in DGCR8 as compared to vehicle treated controls (Figure 6A and B).

Discussion

Since its discovery in DiGeorge Syndrome, a congenital disease caused by a deletion in chromosome 22q11.2 which encodes the *DGCR8* gene, a growing body of literature has detailed a critical role for DGCR8 in canonical miRNA biogenesis (Lambert et al. 2018, Lindsay 2001, Shiohama et al. 2003, Wang et al. 2007). Despite this important progress, our understanding of the mechanisms that control transcriptional regulation of DGCR8 are still not well defined even though it is necessary for proper miRNA biogenesis in virtually all cell types. Our research supports the hypothesis that PADs epigenetically regulate DGCR8 expression in both LßT2 cells and mouse gonadotropes. We report here that citrullination of histone H3 arginine residues 2, 8, and 17 is correlated with a decrease in *Dgcr8* gene expression. As would be predicted, alterations in DGCR8 expression result in downstream effects on miRNA biogenesis.

Khan *et al.* discovered that PAD2 is the predominant isoform expressed in LβT2s and mouse gonadotrope cells and that citrullinated histones are present in the nuclei of both (Khan et al. 2016). In LβT2 cells, citrullination regulates expression of LHβ and FSHβ mRNA, but

not the common alpha subunit (CGA) required for gonadotropin heterodimerization (Khan et al. 2016). Previous studies found that PAD inhibition increases DGCR8 expression in the somatolactotrope derived GH3 cell line (DeVore et al. 2018), so here we investigated if this regulation also occurs in gonadotrope cells since DGCR8 is critical for miRNA biogenesis and knowledge about it in gonadotropes is limited. Using LβT2 cells, we first tested whether PAD inhibition alters expression of the major components of miRNA biogenesis: DGCR8, DROSHA, and DICER. Inhibiting PAD activity in LβT2 cells results in an increase in DGCR8 mRNA, while having no effect on DROSHA or DGCR8. Knockdown of endogenous PAD2 suggests that this isozyme is likely regulating DGCR8 expression. ChIP studies using an anti-citrullinated histone H3 arginine residues 2, 8, and 17 antibody show decreased enrichment of the *Dgcr8* gene following PAD inhibition. Supporting our findings in LßT2 cells, PAD inhibition also results in an increase in DGCR8 expression in dispersed mouse pituitary gonadotrope cells.

Although biogenesis of all miRNAs is likely altered following changes in DGCR8 expression, we chose to examine miR-132 and 212 since they have documented expression and function in gonadotropes (Godoy et al. 2011, Lannes et al. 2016, Lannes et al. 2015). Our results show that following PAD inhibition in LβT2 cells, which increases DGCR8 expression, there is a corresponding decrease pri-miR-132 and 212 as they are processed to their mature counterparts. In contrast, siRNA mediated knockdown of DGCR8 increases pri-miR-132 and 212, since with lower DGCR8 they are not efficiently processed to their mature isoforms. In terms of functional significance, miR-132 and 212 alter target mRNAs Rho GTPase Activating Protein 32 (ARHGAP32) and sirtuin 1 (SIRT1) in LβT2 cells (Godoy et al. 2011, Lannes et al. 2016, Lannes et al. 2015). Fluctuating levels of miR-132 and miR-125b are believed to desensitize LβT2 cells to sustained gonadotropin releasing hormone (GnRH) stimulation (Lannes et al. 2016). Despite these important studies, more work is needed to determine expression patterns of miR-132 and 212 in primary gonadotrope cells over the course of the estrous cycle and to identify the full cohort of downstream mRNA targets, and ultimately, the effect on gonadotrope function.

Estrogen is well documented to regulate PAD2 expression in female reproductive tissues (Horibata et al. 2012, Khan et al. 2016, Takahara et al. 1992). In gonadotropes, Kahn *et al.* showed that PAD2 increases from proestrus to estrus following the increase in serum E2 during the mouse estrous cycle (Khan et al. 2016). If PAD2 is highest during estrus, then it would follow that there would be a corresponding decrease in DGCR8 expression in gonadotropes during estrus and vice versa during diestrus. In pituitaries harvested from mice during diestrus, we found that DGCR8 expression is higher as compared to those from estrus. Supporting this idea, FACS purified gonadotropes enriched from mice and analyzed by RNA-seq show highest expression of DGCR8 during diestrus when serum E2 and PAD2 expression are lowest (Qiao et al. 2016). Our work also shows that E2 treatment of ovariectomized mice results in an increase in PAD2 expression in gonadotropes with a simultaneous decrease in DGCR8. These results suggest an inverse relationship between the expression of PAD2 and DGCR8 in gonadotropes. Work by Wang et al. supports the importance of miRNA biogenesis to gonadotrope function given that cell-specific deletion of DICER suppresses gonadotropins resulting in fertility defects (Wang et al. 2015). Thus,

there is a high likelihood that gonadotrope specific deletion of DGCR8 may have similar fertility defects.

Collectively, our work shows that PAD2 modulates DGCR8 expression in gonadotropes, which is necessary for miRNA biogenesis. Future studies are necessary to help uncover the relationship between DGCR8, miRNA, and target mRNA expression patterns in gonadotropes during different phases of the estrous cycle. In conclusion, we suggest that a PAD2/DGCR8/miRNA mechanism contributes to gonadotrope cell physiology, and ultimately, may provide novel targets to control fertility and reproduction.

Funding

Research reported in this publication was supported by the National Institute of General Medical Sciences and the Eunice Kennedy Shriver National Institute of Child Health and Human Development of the National Institutes of Health under Award Numbers P20GM103432 and R21HD090541, respectively. The content is solely the responsibility of the authors and does not necessarily represent the official views of the National Institutes of Health.

References

Ahmed K, LaPierre MP, Gasser E, Denzler R, Yang Y, Rulicke T, Kero J, Latreille M and Stoffel M (2017) Loss of microRNA-7a2 induces hypogonadotropic hypogonadism and infertility. J Clin Invest, 127(3), pp. 1061–1074. [PubMed: 28218624]

Beezhold KJ, Castranova V and Chen F (2010) Microprocessor of microRNAs: regulation and potential for therapeutic intervention. Mol Cancer, 9, pp. 134. [PubMed: 20515486]

Bicker KL and Thompson PR The protein arginine deiminases: Structure, function, inhibition, and disease. Biopolymers, 99(2), pp. 155–63. [PubMed: 23175390]

Cherrington BD, Zhang X, McElwee JL, Morency E, Anguish LJ and Coonrod SA (2012) Potential role for PAD2 in gene regulation in breast cancer cells. PLoS One, 7(7), pp. e41242. [PubMed: 22911765]

Christensen AO, Li G, Young CH, Snow B, Khan SA, DeVore SB, Edwards S, Bouma GJ, Navratil AM, Cherrington BD, et al. (2022) Peptidylarginine deiminase enzymes and citrullinated proteins in female reproductive physiology and associated diseasesdagger. Biol Reprod, 107(6), pp. 1395–1410. [PubMed: 36087287]

DeVore SB, Young CH, Li G, Sundararajan A, Ramaraj T, Mudge J, Schilkey F, Muth A, Thompson PR and Cherrington BD (2018) Histone Citrullination Represses MicroRNA Expression, Resulting in Increased Oncogene mRNAs in Somatolactotrope Cells. Mol Cell Biol, 38(19).

Godoy J, Nishimura M and Webster NJ (2011) Gonadotropin-releasing hormone induces miR-132 and miR-212 to regulate cellular morphology and migration in immortalized LbetaT2 pituitary gonadotrope cells. Mol Endocrinol, 25(5), pp. 810–20. [PubMed: 21372146]

Gregory RI, Yan KP, Amuthan G, Chendrimada T, Doratotaj B, Cooch N and Shiekhattar R (2004) The Microprocessor complex mediates the genesis of microRNAs. Nature, 432(7014), pp. 235–40. [PubMed: 15531877]

Gyorgy B, Toth E, Tarcsa E, Falus A and Buzas EI (2006) Citrullination: a posttranslational modification in health and disease. Int J Biochem Cell Biol, 38(10), pp. 1662–77. [PubMed: 16730216]

Ha M and Kim VN (2014) Regulation of microRNA biogenesis. Nat Rev Mol Cell Biol, 15(8), pp. 509–24. [PubMed: 25027649]

Hasuwa H, Ueda J, Ikawa M and Okabe M (2013) miR-200b and miR-429 function in mouse ovulation and are essential for female fertility. Science, 341(6141), pp. 71–3. [PubMed: 23765281]

Horibata S, Coonrod SA and Cherrington BD (2012) Role for peptidylarginine deiminase enzymes in disease and female reproduction. J Reprod Dev, 58(3), pp. 274–82. [PubMed: 22790870]

Khan SA, Edwards BS, Muth A, Thompson PR, Cherrington BD and Navratil AM (2016) GnRH Stimulates Peptidylarginine Deiminase Catalyzed Histone Citrullination in Gonadotrope Cells. Mol Endocrinol, 30(10), pp. 1081–1091. [PubMed: 27603413]

Knight JS, Subramanian V, O'Dell AA, Yalavarthi S, Zhao W, Smith CK, Hodgin JB, Thompson PR and Kaplan MJ (2015) Peptidylarginine deiminase inhibition disrupts NET formation and protects against kidney, skin and vascular disease in lupus-prone MRL/lpr mice. Ann Rheum Dis, 74(12), pp. 2199–206. [PubMed: 25104775]

Lambert MP, Arulselvan A, Schott A, Markham SJ, Crowley TB, Zackai EH and McDonald-McGinn DM (2018) The 22q11.2 deletion syndrome: Cancer predisposition, platelet abnormalities and cytopenias. Am J Med Genet A, 176(10), pp. 2121–2127. [PubMed: 28940864]

Lannes J, L'Hote D, Fernandez-Vega A, Garrel G, Laverriere JN, Cohen-Tannoudji J and Querat B (2016) A regulatory loop between miR-132 and miR-125b involved in gonadotrope cells desensitization to GnRH. Sci Rep, 6, pp. 31563. [PubMed: 27539363]

Lannes J, L'Hote D, Garrel G, Laverriere JN, Cohen-Tannoudji J and Querat B (2015) Rapid communication: A microRNA-132/212 pathway mediates GnRH activation of FSH expression. Mol Endocrinol, 29(3), pp. 364–72. [PubMed: 25635942]

Lindsay EA (2001) Chromosomal microdeletions: dissecting del22q11 syndrome. Nat Rev Genet, 2(11), pp. 858–68. [PubMed: 11715041]

Mohanan S, Cherrington BD, Horibata S, McElwee JL, Thompson PR and Coonrod SA (2012) Potential role of peptidylarginine deiminase enzymes and protein citrullination in cancer pathogenesis. Biochem Res Int, 2012, pp. 895343. [PubMed: 23019525]

Navratil AM, Knoll JG, Whitesell JD, Tobet SA and Clay CM (2007) Neuroendocrine plasticity in the anterior pituitary: gonadotropin-releasing hormone-mediated movement in vitro and in vivo. Endocrinology, 148(4), pp. 1736–44. [PubMed: 17218416]

Qiao S, Nordstrom K, Muijs L, Gasparoni G, Tierling S, Krause E, Walter J and Boehm U (2016) Molecular Plasticity of Male and Female Murine Gonadotropes Revealed by mRNA Sequencing. Endocrinology, 157(3), pp. 1082–93. [PubMed: 26677881]

Schneider CA, Rasband WS and Eliceiri KW (2012) NIH Image to ImageJ: 25 years of image analysis. Nat Methods, 9(7), pp. 671–5. [PubMed: 22930834]

Shiohama A, Sasaki T, Noda S, Minoshima S and Shimizu N (2003) Molecular cloning and expression analysis of a novel gene DGCR8 located in the DiGeorge syndrome chromosomal region. Biochem Biophys Res Commun, 304(1), pp. 184–90. [PubMed: 12705904]

Takahara H, Kusubata M, Tsuchida M, Kohsaka T, Tagami S and Sugawara K (1992) Expression of peptidylarginine deiminase in the uterine epithelial cells of mouse is dependent on estrogen. J Biol Chem, 267(1), pp. 520–5. [PubMed: 1730614]

Vossenaar ER, Zendman AJ, van Venrooij WJ and Pruijn GJ (2003) PAD, a growing family of citrullinating enzymes: genes, features and involvement in disease. Bioessays, 25(11), pp. 1106–18. [PubMed: 14579251]

Wang H, Graham I, Hastings R, Gunewardena S, Brinkmeier ML, Conn PM, Camper SA and Kumar TR (2015) Gonadotrope-specific deletion of Dicer results in severely suppressed gonadotropins and fertility defects. J Biol Chem, 290(5), pp. 2699–714. [PubMed: 25525274]

Wang Y, Medvid R, Melton C, Jaenisch R and Blelloch R (2007) DGCR8 is essential for microRNA biogenesis and silencing of embryonic stem cell self-renewal. Nat Genet, 39(3), pp. 380–5. [PubMed: 17259983]

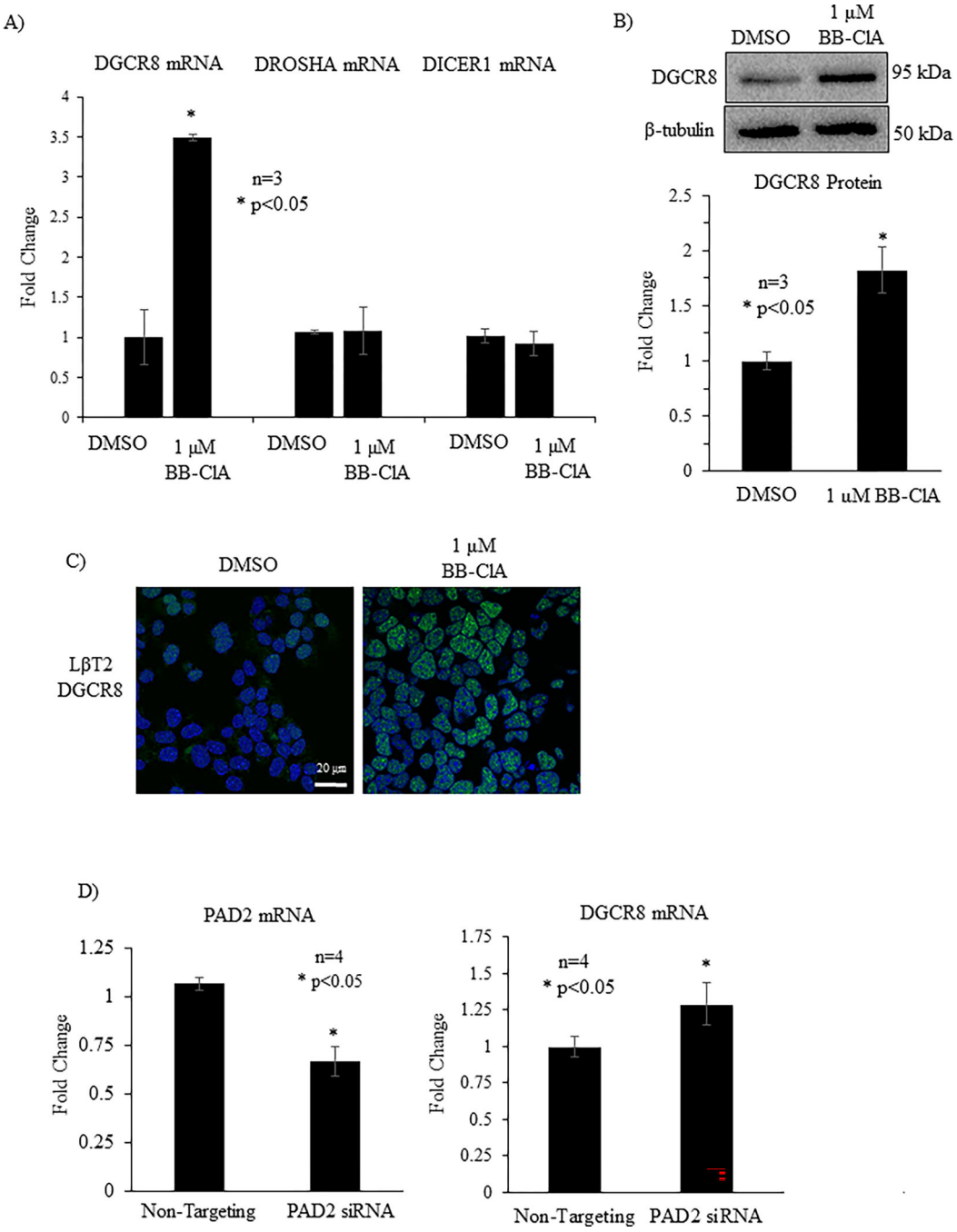

Figure 1:

PAD Inhibition Alters DGCR8 mRNA and Protein Expression in LβT2 cells. (A) LßT2 cells were treated with vehicle (DMSO) or 1 μM BB-ClA for 12 hours then examined by qPCR with intron spanning primers for DGCR8, DROSHA, and DICER. All values are expressed as means ± SEM. Means were separated using Student's t-test (n=3, * p<0.05). (B) Following the same treatment paradigm, LβT2 cell lysates were examined by western blot and membranes probed with an anti-DGCR8 antibody or anti-β-tubulin as a loading control. The top panel shows a representative western blot, while the graph below represents

the quantification of multiple western blots using BioRad Image Lab 4.0. Data are presented as means ± SEM and separated using Student's t-test (n=3, * $p<0.05$). (C) LßT2 cells were grown on glass bottom dishes overnight then treated as described above. Cells were examined by immunocytochemistry using an anti-DGCR8 antibody (green) and stained with DAPI (blue) and imaged using a Zeiss LSM 710 confocal microscope using a 40X objective and scale bar is 20 μm. (D) LβT2 cells were transfected with 25 nM non-targeting or PAD2 siRNAs for 48 hours, then examined by qPCR with intron spanning primers for PAD2 and DGCR8. All values are expressed as means ± SEM. Means were separated using Student's t-test (n=4, * $p<0.05$).

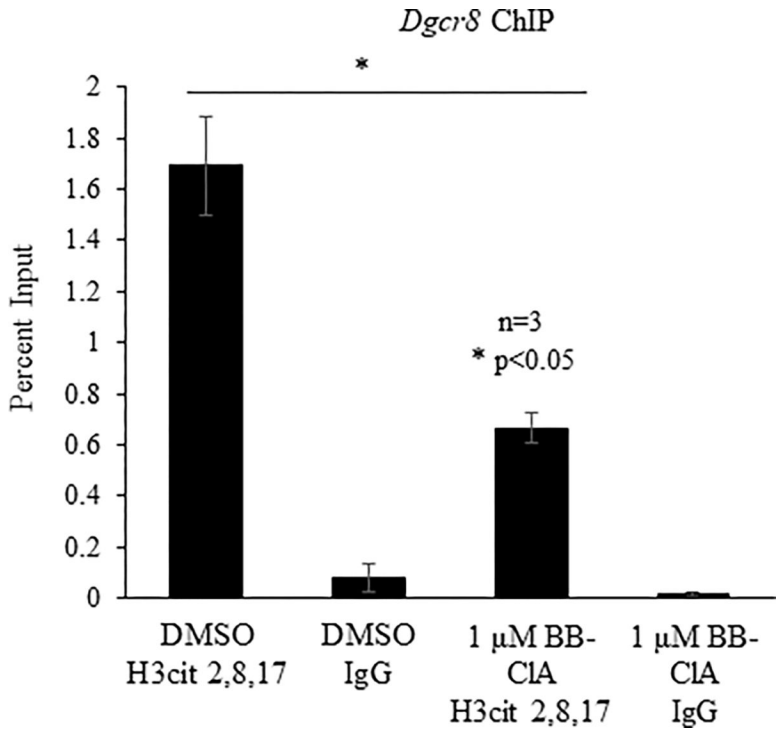

Figure 2:

Citrullinated histones are directly associated with the *Dgcr8* gene. LßT2 cells were treated with vehicle (DMSO) or 1 µM BB-ClA for 12 hours. Cross-linked histone-DNA complexes were immunoprecipitated with an anti-histone H3Cit 2,8,17 antibody or nonspecific IgG as the negative control, then examined by qPCR with primers specific for the mouse *Dgcr8* gene. Results were analyzed using the percent input method, and all values are means ± SEM. Means were separated using a Student's t-test (n=3, * $p<0.05$).

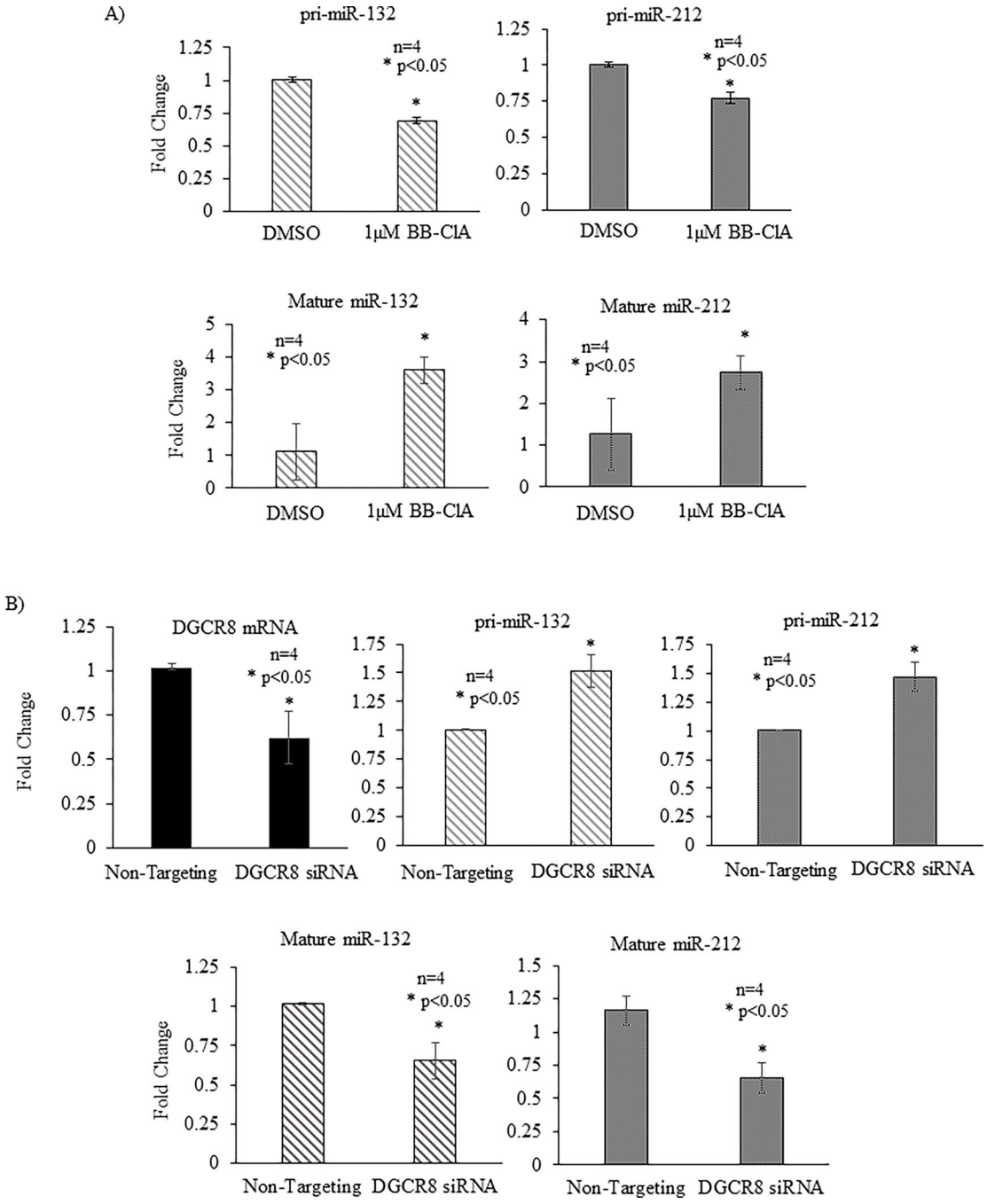

Figure 3:

PAD inhibition and DGCR8 knockdown alter miR-132 and 212 biogenesis in LβT2 cells. (A) LβT2 cells were treated with vehicle (DMSO) or 1 μM BB-ClA for 12 hours, then examined by qPCR using primers for pri-miR-132 and 212 and Taqman miRNA assays for miR-132 and 212. All values are expressed as means ± SEM. Means were separated using Student's t-test (n=4, * p<0.05). (B) LβT2 cells were transfected with 25 nM non-targeting or DGCR8 siRNAs for 48 hours then examined by qPCR for DGCR8 and pri and mature

miR-132 and 212. All values are expressed as means ± SEM, and means were separated using Student's t-test (n=4, * $p<0.05$).

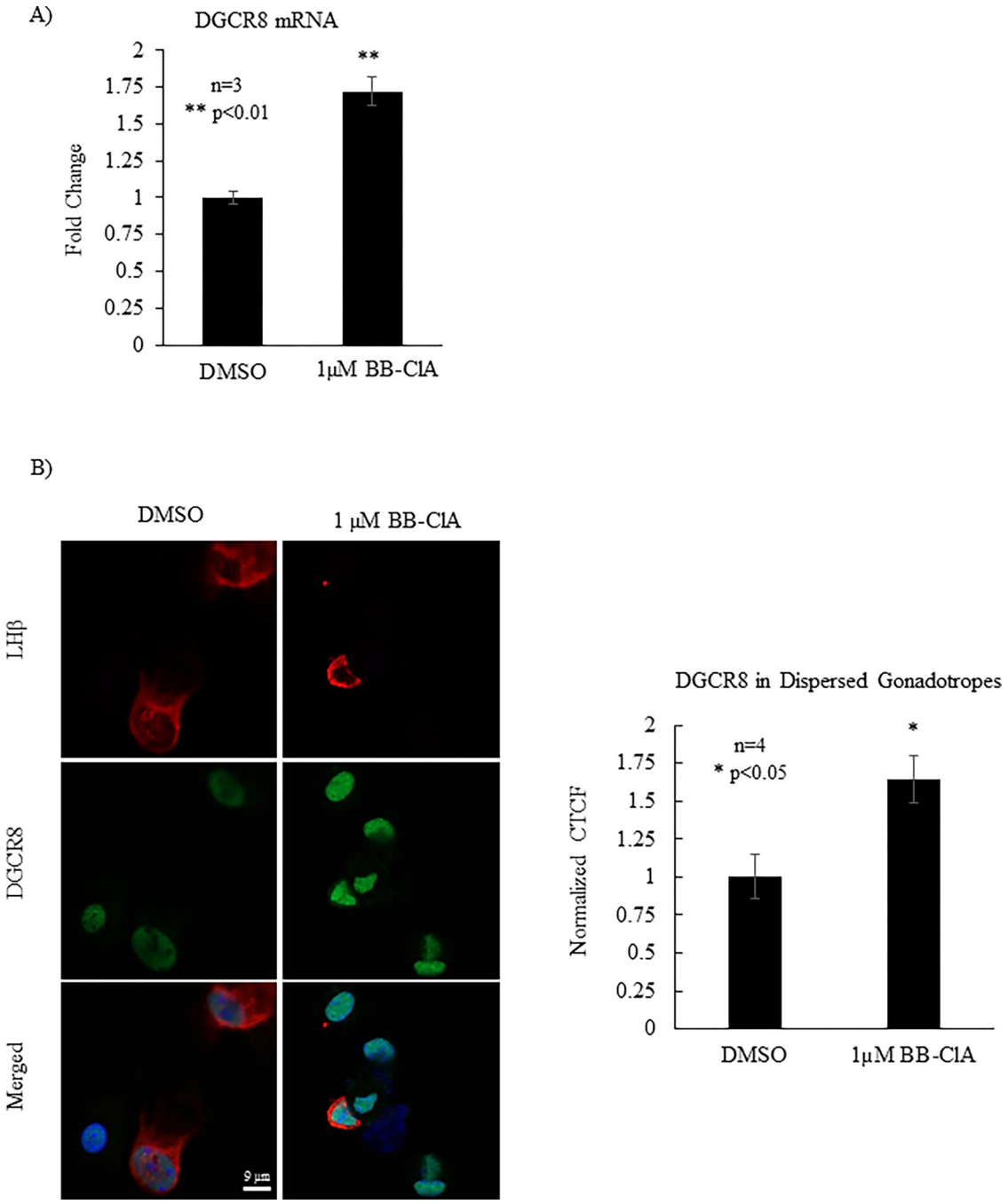

Figure 4:

PAD Inhibition increases DGCR8 expression in dispersed mouse gonadotropes. (A) Mouse pituitary cells were treated with vehicle (DMSO) or 1 μM BB-ClA for 12 hours, then examined by qPCR with intron spanning primers for DGCR8. All values are expressed as means ± SEM, and means were separated using Student's t-test with * indicating significant differences (n=3, ** p<0.01). (B) Mouse pituitaries were dispersed, plated in glass bottom dishes overnight, and then treated as described above. Cells were then examined by immunocytochemistry using anti-DGCR8 (green) and anti-LHβ (red) antibodies and stained

with DAPI (blue). Cells were imaged using a Zeiss LSM 980 confocal microscope using a 63X objective and scale bar is 9 μm. Representative images are shown on the left and ImageJ was used to calculate the average normalized corrected total cell fluorescence (CTCF) of DGCR8 in gonadotrope nuclei for the graph on the right. All values are expressed as means ± SEM. Means were separated using Student's t-test with * indicating significant differences (n=4, * $p < 0.05$).

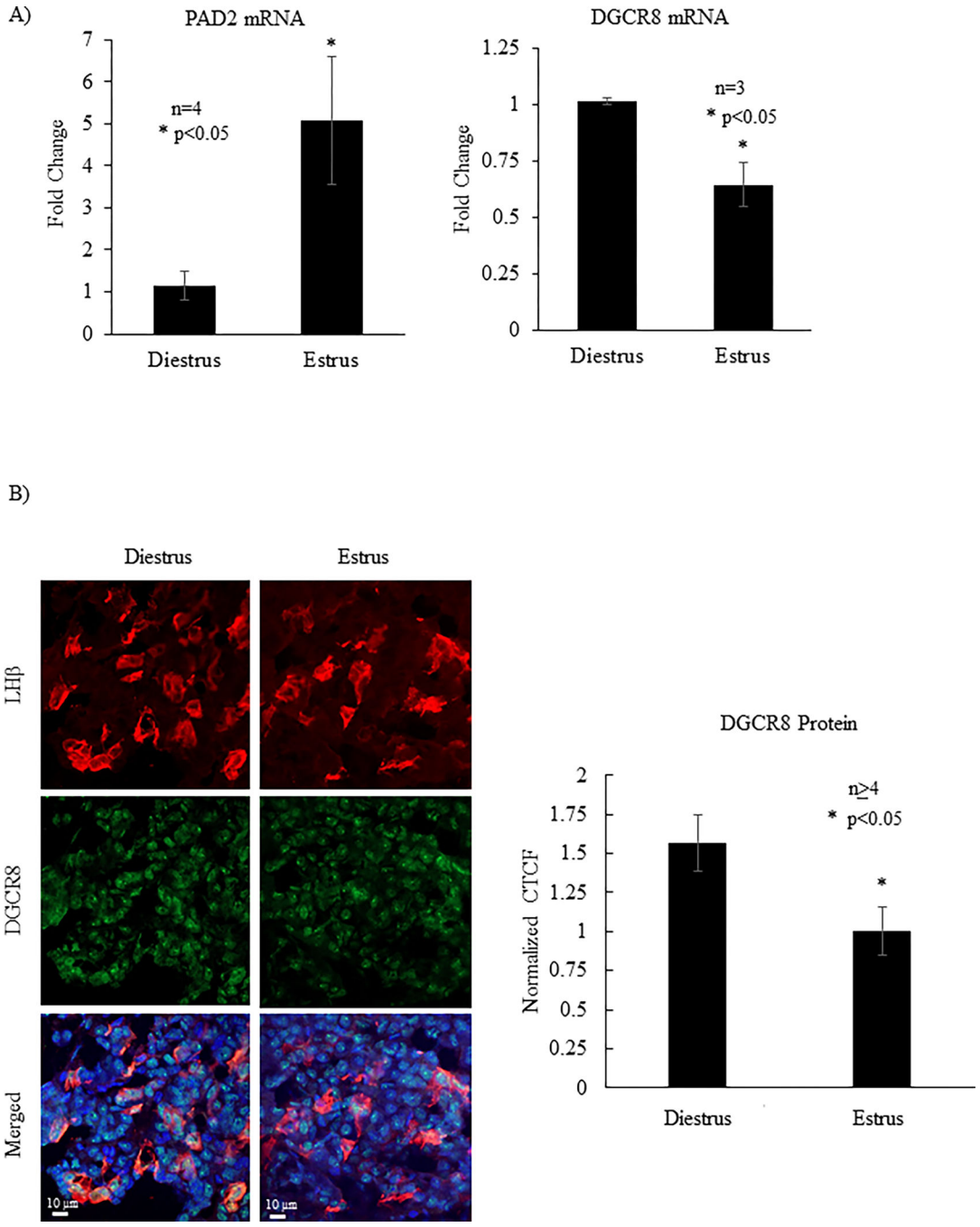

Figure 5:

DGCR8 expression in mouse gonadotropes is highest during diestrus. (A) Mice were estrous cycle staged using vaginal cytology, pituitary glands collected during diestrus and estrus, and PAD2 and DGCR8 expression measured by qPCR. All values are expressed as means ± SEM. Means were separated using Student's t-test with * indicating significant differences (n≥3, * p<0.05). (B) Whole pituitary glands were collected during diestrus and estrus. Mouse pituitaries sections were examined by immunocytochemistry using anti-DGCR8 (green) and anti-LHβ (red) antibodies and stained with DAPI (blue). Cells were imaged

using a Zeiss LSM 910 confocal microscope using a 63X objective and scale bar is 10 μm. Representative images are shown on the left and ImageJ was used to calculate the average CTCF of DGCR8 in gonadotrope nuclei during estrus and diestrus. All values are expressed as means ± SEM. Means were separated using Student's t-test with * indicating significant differences (n=5 for diestrus, n=4 for estrus * $p<0.05$).

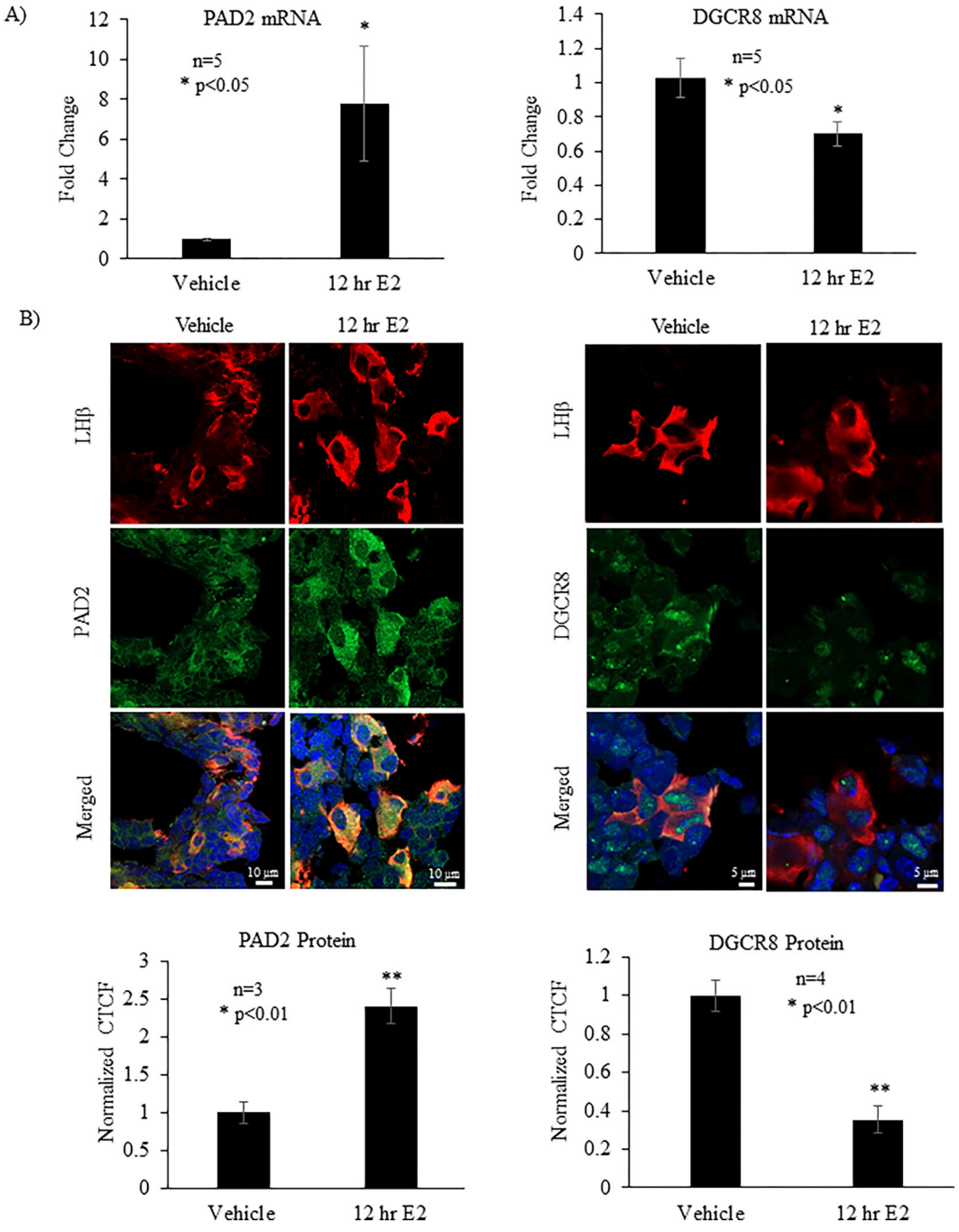

Figure 6:

17β-estradiol treatment of ovariectomized mice results in an increase in PAD2 expression in gonadotropes with a corresponding decrease in DGCR8. (A) Following 12 hours of vehicle or E2 treatment, mouse pituitaries were examined by qPCR with primers for PAD2 and DGCR8. All values are expressed as means ± SEM. Means were separated using Student's t-test with * indicating significant differences (n=5, * p<0.05). (B). Following treatment described above, pituitary sections were examined by immunocytochemistry using anti-PAD2 or DGCR8 (green) and anti-LHβ (red) antibodies and stained with DAPI (blue).

Cells were imaged using a Zeiss LSM 910 confocal microscope using a 63X objective and scale bar is 5 or 10 μm. Representative images are shown on the top and ImageJ was used to calculate the average CTCF of PAD2 (whole cell) and DGCR8 (nuclei) in gonadotropes. All values are expressed as normalized means ± SEM and ≥12 gonadotropes were quantified per pituitary from different sections. Means were separated using Student's t-test with ** indicating significant differences (n=3 for vehicle and n=4 for E2 ** $p<0.01$).